A neutron diffraction study of the order - disorder phase transition in sodium nitrate

1997 J. Phys.: Condens. Matter 9 2423

(http://iopscience.iop.org/0953-8984/9/11/010)

J. Phys.: Condens. Matter **9** (1997) 2423–2432. Printed in the UK PII: S0953-8984(97)78325-5

A neutron diffraction study of the order–disorder phase transition in sodium nitrate

S J Payne†, M J Harris‡, M E Hagen† and M T Dove§

† Department of Physics, Keele University, Keele, Staffordshire ST5 5BG, UK
‡ ISIS Facility, Rutherford Appleton Laboratory, Chilton, Didcot, Oxon OX11 0QX, UK
§ Department of Earth Sciences, Downing Street, University of Cambridge, Cambridge CB2 3EQ, UK

Received 2 October 1996

Abstract. The temperature dependence of the critical scattering above T_c and the order parameter below T_c have been measured for sodium nitrate ($NaNO_3$) using time-of flight neutron diffraction. Sodium nitrate undergoes a structural phase transition from a low-temperature rhombohedral $R\bar{3}c$ structure to a high-temperature $R\bar{3}m$ structure which is characterized by the disappearance of superlattice reflections at positions corresponding to the Z point of the high-temperature Brillouin zone. In the critical region below $T_c = 548.74 \pm 0.47$ K the order parameter displays a crossover behaviour. For temperatures $T < T_L \approx 543$ K the temperature dependence of the order parameter can be described by a power law in the effective reduced temperature $t^* = |T_c^* - T|/T_c^*$ with $\beta = 0.22 \pm 0.02$ and an effective critical temperature $T_c^* = 551.02 \pm 0.54$ K. However, for temperatures $T_L < T < T_c$ the temperature dependence of the order parameter follows a power law in the reduced temperature $t = |T_c - T|/T_c$ with $\beta = 0.41 \pm 0.02$. At temperatures $T > T_c$ the critical scattering takes the usual form of a Lorentzian lineshape, and the correlation length and susceptibility can be described by power-law equations in the reduced temperature with the exponents $\nu = 0.65 \pm 0.05$ and $\gamma = 1.27 \pm 0.04$ respectively. There is a second Lorentzian lineshape in the diffraction pattern above T_c which is much wider than the Lorentzian describing the critical scattering and is essentially independent of temperature.

1. Introduction

In this paper we report the results of a neutron diffraction study of the order–disorder structural phase transition in sodium nitrate ($NaNO_3$). This transition occurs at a temperature of ∼549 K and is from a low-temperature $R\bar{3}c$ crystal structure to a high-temperature $R\bar{3}m$ structure [1]. There has been a lot of the interest in this phase transition because of its similarity to the high-temperature transition in calcite ($CaCO_3$) [2] which is of considerable geological importance. The $R\bar{3}c \rightarrow R\bar{3}m$ symmetry change is marked in a diffraction experiment by the disappearance of superlattice reflections at wavevectors corresponding to the Z points of the high-temperature Brillouin zone. In a hexagonal-unit-cell description these are (h, k, l) reflections for which l is odd [1]. The change in symmetry is due to a rotational disordering of the molecular nitrate groups by 60° flips about the trigonal c-axis.

An x-ray study of the temperature dependence of the $(\bar{1}, 2, 3)$ Bragg peak in sodium nitrate by Schmahl and Salje [3] suggested that the underlying character of this phase transition was tri-critical. A tri-critical transition is one which is on the borderline between discontinuous (first-order) and continuous (second-order) behaviour [4]. For temperatures

0953-8984/97/112423+10$19.50

in the range 280 K to 460 K, Schmahl and Salje found that the order parameter derived from this Bragg peak was governed by a critical exponent $\beta = 0.25$ [3], which is the standard tri-critical value [4]. A similar order parameter exponent was found for calcite by Dove and Powell [2] in a neutron powder diffraction experiment. However, in the temperature range 460 K $< T < T_c$ (=552.4 K), Schmahl and Salje found that the β-exponent in sodium nitrate was reduced from the value of 0.25 to $\beta = 0.22 \pm 0.01$. It was speculated [3, 5] that this change in the β-value was associated with excitations into an incipient phase which had a monoclinic structure. There was some theoretical support for this speculation from computer simulation work [6] which suggested that diffuse scattering, which had been observed in x-ray diffraction experiments [7] at wavevectors corresponding to the F points of the high-temperature Brillouin zone, was due to these excitations. A detailed measurement [8] of the temperature dependence of this x-ray diffuse scattering, however, showed that it could be explained by the temperature dependence of the transverse acoustic phonons (as measured by inelastic neutron scattering [9]) at this position. There is, however, evidence from an inelastic neutron scattering study of calcite for the existence of these excitations into another structure at these F-point positions in calcite [10, 11].

The initial aim of the experiments reported here was to examine the critical scattering associated with the Z-point structural phase transition in sodium nitrate and to determine the critical exponents ν and γ for comparison with the β-exponent of Schmahl and Salje. In doing this we have also measured the temperature dependence of the order parameter close to T_c.

2. Experimental details

The neutron diffraction measurements were carried out on a single crystal of sodium nitrate using the PRISMA spectrometer at the ISIS Spallation Neutron Source, Rutherford Appleton Laboratory, UK. In the work reported in this paper, PRISMA was operated as a multi-detector single-crystal diffractometer with Soller collimation in front of each of the detectors in the detector bank. This was achieved by removing the analyser crystals from four detectors and allowing these detectors to each view the sample directly through their individual collimators. The crystal had a volume of 1 cm^3 and was oriented so that the $(H, H, 0)$ and $(0, 0, L)$ reciprocal-lattice vectors were in the scattering plane. It was secured to the end of a stainless steel peg using a thin aluminium strap, and the peg was then attached to the centre stick of a vacuum furnace. The peg and end of the centre stick were shielded from the neutron beam using gadolinium foil. The temperature of the sample was measured using a K-type thermocouple placed near to the sample and recorded every 30 seconds by the spectrometer control computer. The temperature stability for the duration of each run (up to 100 minutes) was better than ± 0.3 K. All of the temperature changes were performed in small steps with the furnace controls set to ensure a gentle heating of the crystal. This was necessary because the melting point of the crystal is only $\sim$20 K above the transition temperature [8], so any large temperature overshoot from the furnace could melt or at least cause irreversible damage to the crystal.

3. Experimental results

The results of our measurements on $NaNO_3$ are given in the following two subsections. Subsection 3.1 describes the measurements of the (1, 1, 3) superlattice reflection below T_c and subsection 3.2 describes how the critical scattering data were collected and analysed.

3.1. Bragg peak data ($T < T_c$)

Measurements were made of the temperature dependence of the (1, 1, 3) superlattice reflection using a single detector set to a scattering angle of -60° with respect to the incident neutron beam. The integrated intensity at the Bragg peak position was recorded at a total of 27 temperatures in the range from 525.90 K to 549.14 K. At each temperature scans were performed by rocking the crystal through a rotation angle of $\pm 1^\circ$ about the angle which corresponded to the (1, 1, 3) Bragg peak in 21 steps of 0.1°. The integrated intensity of the Bragg peak was then found by integrating the spectra over both the time of flight of the neutrons from 5500 μs to 6500 μs, and the crystal rotation angle. We note that at a scattering angle of $\phi = -60^\circ$, the (1, 1, 3) Bragg peak occurred at a flight time of 5791 μs.

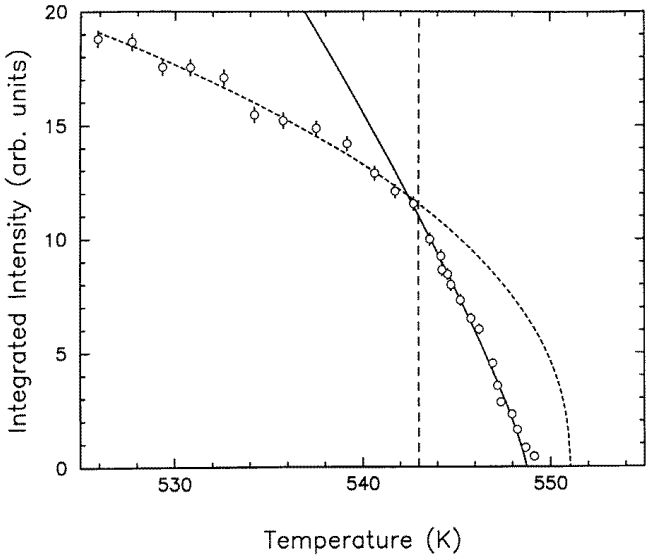

Figure 1. The integrated intensity of the (1, 1, 3) superlattice peak in the range 525.90 K to 549.14 K. The vertical dashed line shows the approximate position of the crossover temperature T_L described in the text. The solid line is the result of the power-law fit of the data at temperatures $T > T_L$ to equation (5) and the short-dashed line is the result of the power-law fit of the data at temperatures $T < T_L$ to equation (5). See the text.

Figure 1 shows the results for the integrated intensity as a function of temperature. It can be seen that there is distinctly different behaviour either side of a temperature $T_L \sim 543$ K. Although primary extinction must always be a concern when measuring the β-exponent from a Bragg peak intensity [12, 13], our measurements were performed at reduced temperatures very close to T_c where the Bragg peak intensity is weak, and it is therefore unlikely that extinction could cause this change in behaviour. Another effect which can distort a measurement of the Bragg intensity is detector saturation [13] and so we were careful to ensure that this did not occur during these measurements. This change in behaviour at T_L is significant since, as will be discussed in sections 4.1 and 4.2, it means that the Bragg peak intensity could not be described by a single β-exponent over the whole of the temperature range shown in figure 1.

3.2. Critical scattering data ($T > T_c$)

The critical scattering data were collected using four of the sixteen detectors on the PRISMA spectrometer, set up in diffraction mode [13]. This arrangement allows four radial scans to be made through reciprocal space for any angular setting of the crystal. If the crystal is then rotated in small increments these groups of four radial scans can be merged together to cover any feature as required. This technique is described more fully in references [13] and [14]. For each temperature, a total of 15 angular settings of the crystal were used, giving a total of 60 radial time-of-flight scans covering the region around the (1, 1, 3) position in reciprocal space where the critical scattering occurs.

The raw time-of-flight scans were transformed using the program VCRS [15] such that each radial scan represented a path in the wavevector transfer $\boldsymbol{Q}$ covering the range from $Q = 2.2$ to 3.2 Å^{-1} in 0.01 Å^{-1} steps, a total of 100 divisions. This gave an overall grid of 6000 data points covering the critical scattering. The VCRS program carries out the relevant normalization procedures for the data [13, 15], accounting for the variation of the incident neutron flux with energy and correcting for the different efficiencies of the four detectors using a calibration spectrum taken from a standard vanadium incoherent scatterer.

Each of the 6000 data points in the grid is the result of a convolution of the structure factor for the critical scattering which was centred at the (1, 1, 3) position, and the resolution function of the PRISMA spectrometer, centred at that particular data point. The structure factor for the critical scattering $S(\boldsymbol{Q})$ used in the data analysis was modelled by a Lorentzian function [12, 17] given by

$$S(\boldsymbol{Q}) = \frac{\chi_0}{1 + ((Q_L - Q_L^0)/\kappa_c)^2 + \left[((Q_H - Q_H^0)^2 + Q_V^2)/\kappa_{ab}^2\right]} \tag{1}$$

where Q_L, Q_H and Q_V respectively represent the wavevector components along the $(0, 0, L)$ and $(H, H, 0)$ directions in the scattering plane, and the $(\bar{H}, H, 0)$ direction vertically out of the scattering plane. This function is centred on the position $Q_L^0 = 3$ and $Q_H^0 = 1$, its height χ_0 is equal to the susceptibility, and there are two inverse correlation lengths κ_c and κ_{ab} to allow for the possibility of different (anisotropic) behaviours along the c^*-axis and in the a^*–b^* plane. The convolution of this structure factor with the resolution function and the non-linear least-squares fitting to the data were carried out using the CRTFIT program [13]. The resolution function formalism which is used in this program has been described in references [13], [14] and [16] and the fitting procedure in references [13] and [14]. The collimation and neutron pulse lineshape parameters used in calculating the values of the resolution function were the same as those given in table (A.1) of reference [14] except for the sample mosaic spread parameter which was given by a value $f_{sh} = f_{sv} = 0.18^\circ$. It should be noted that these parameters accurately predicted the measured widths of the (1, 1, 3) Bragg peak below T_c.

Table 1. The parameters describing the wide temperature-independent Lorentzian used in the fitting process as described in the text.

χ_0	κ_{ab}	κ_c
0.012 ± 0.002	0.052 ± 0.004	0.602 ± 0.050

Above T_c the critical scattering was measured at nine temperatures from 551.14 K to 558.22 K. In order to obtain satisfactory fits to the measured scattering over the whole temperature range it was necessary to use two Lorentzian lineshapes (both of them of the

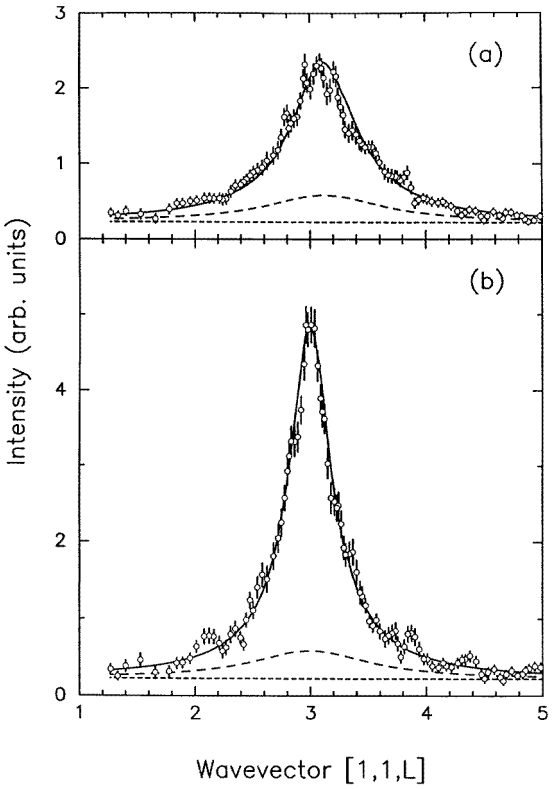

Figure 2. Cuts through the critical scattering data along the $(1, 1, L)$ direction at temperatures of (a) 557.09 K and (b) 552.65 K are shown. The solid lines are the best fits to the two Lorentzian lineshapes as described in the text. The short-dashed line is the background level and the long-dashed line is the wide Lorentzian lineshape described in the text.

Table 2. The values for the critical exponent β and transition temperature describing the behaviour of the order parameter in the two temperature ranges below T_c.

Temperature range	Exponent β	Amplitude I_0	T_c (K)
$T < T_L$	0.22 ± 0.02	74.3 ± 0.5	551.02 ± 0.54
$T_L < T < T_c$	0.41 ± 0.02	469 ± 38	548.74 ± 0.47

form described by equation (1)). Although both Lorentzians and the background level were initially allowed to vary in the fitting procedure, the values returned for one of the Lorentzians and the background level were effectively independent of temperature. This 'temperature-independent' Lorentzian was much wider and of lower height than the other Lorentzian whose width and height varied significantly with temperature. We therefore assumed that the scattering represented by the wide (temperature-independent) Lorentzian results from non-critical fluctuations, while the scattering represented by the narrower (temperature-dependent) Lorentzian results from the true critical scattering. Consequently the data were fitted again with the wide Lorentzian, and background levels held fixed at their average values from the free fits. These average values describing the wide Lorentzian

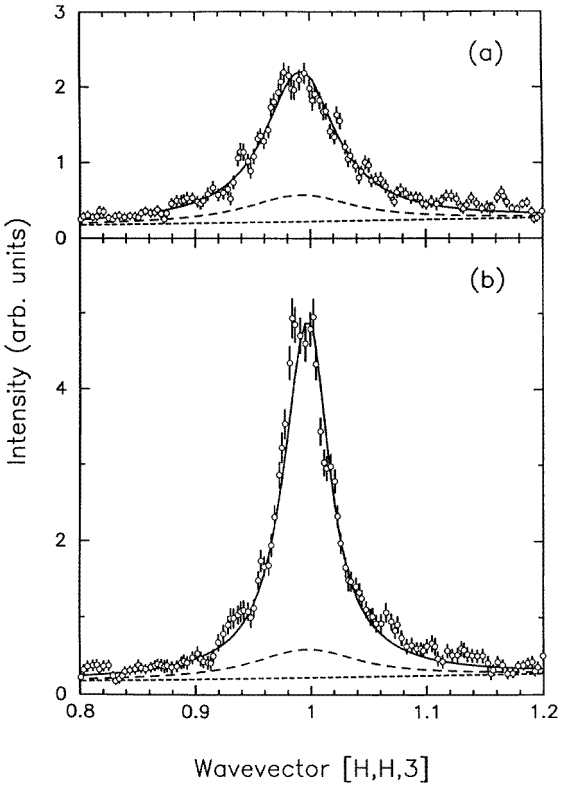

Figure 3. Cuts through the critical scattering data along the $(H, H, 3)$ direction at temperatures of (a) 557.09 K and (b) 552.65 K are shown. The solid lines are the best fits to the two Lorentzian lineshapes as described in the text. The short-dashed line is the background level and the long-dashed line is the wide Lorentzian lineshape described in the text.

are given in table 1. The resulting fits to the measured scattering had agreement factors [14] in the range 1.07 to 1.15. In figures 2(a) and 2(b) we show cuts through the grids of experimental data and best-fit calculated values (solid lines) along the $(1, 1, L)$ direction at temperatures of (a) 557.09 K and (b) 552.65 K. Figures 3(a) and 3(b) are the equivalent cuts along the $(H, H, 3)$ direction. In these figures the background level is shown by a short-dashed line, and the wide (temperature-independent) Lorentzian by a long-dashed line.

4. Discussion

The conventional picture of a continuous phase transition is one in which the order parameter (M), inverse correlation length (κ) and susceptibility (χ) all obey power-law equations of the form (see, for example, references [17, 18])

$$M = M_0 t^{\beta} \tag{2}$$

$$\kappa = \kappa_0 t^{\nu} \tag{3}$$

$$\chi = \chi_0 t^{-\gamma} \tag{4}$$

where $t = |T - T_c| / T_c$ is the reduced temperature. On approaching T_c from below the order parameter falls smoothly to zero with a single critical exponent β. In a neutron diffraction experiment the Bragg peak intensity is proportional to the square of the order parameter and so should obey the power law given by [12, 17]

$$I \propto M^2 \Rightarrow I = I_0 t^{2\beta}. \tag{5}$$

On approaching T_c from above, the inverse correlation length, which is the half-width of the structure factor for the critical scattering (cf. equation (1)), should fall smoothly to zero while the susceptibility should smoothly diverge. This should all occur with a value of T_c which is common to I, κ and χ. The results that we have obtained from sodium nitrate, however, do not conform precisely with this conventional picture.

We will discuss our results in terms of three temperature regions (1) $T < T_L$, (2) $T_L < T < T_c$ and (3) $T > T_c$, where the temperature $T_L \approx 543$ K is indicated in figure 1 by the vertical dashed line.

4.1. Temperatures $T < T_L$

In this temperature range the Bragg peak intensity data were fitted to the power law given in equation (5) with both β and T_c as variables. The best-fit result was $\beta = 0.22 \pm 0.02$ with an effective transition temperature of $T_c^* = 551.02 \pm 0.54$ K which is shown in figure 1 by the dashed line. This result for β is in good agreement with the result of Schmahl and Salje [3] who, as noted earlier, found from an x-ray diffraction study of the temperature dependence of the $(\bar{1}, 2, 3)$ Bragg peak that in the temperature range 460 K to $T_c = 552.4$ K the value of β was 0.22 ± 0.01.

4.2. Temperatures $T_L < T < T_c$

The data for the integrated intensity at the (1, 1, 3) Bragg peak position in this temperature range were again fitted to the power law given by equation (5) with β and T_c variable. In doing such a fit of the integrated intensity close to T_c one must be careful not to include the effect of critical scattering [12, 13]. An estimate of the contribution of the critical scattering to the integrated intensity could be made because some of the critical scattering style measurements (cf. section 3.2) were made at temperatures close to but below T_c. These runs were analysed in the same way as those for $T > T_c$ except that a resolution-limited Gaussian peak was also added to represent the Bragg peak. From these fit results for the two Lorentzians and the Bragg peak we could then calculate the relative contributions of Bragg peak and critical scattering in the integrated intensity scans through the Bragg peak position. Consequently we excluded data points above 548.20 K where the critical scattering made a significant contribution to the integrated intensity. The best fit was given by a β-exponent of 0.41 ± 0.02 and a transition temperature of $T_c = 548.74 \pm 0.47$ K. The result of this fit is shown by the solid line in figure 1 and summarized in table 2 along with the fit results described in section 4.1. We note that in the x-ray experiment carried out by Schmahl and Salje [3] there were only three data points at temperatures in the range $T_L < T < T_c$ (cf. figure 7 of reference [3]). There is therefore no discrepancy between our result for this temperature range and their result; it is simply that our result corresponds to a smaller range of reduced temperature.

The change in behaviour at $T_L \approx 543$ K is quite dramatic, and although it may be obvious from the data shown in figure 1 it is worth noting that we were unable to satisfactorily fit the data over the whole range from 525.90 K to 548.20 K with the power

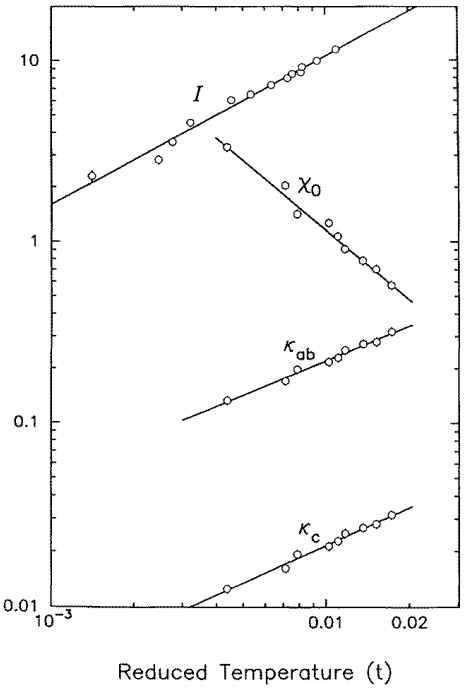

Figure 4. A log–log plot of the temperature dependence of (a) κ_c, (b) κ_{ab}, (c) the susceptibility χ_0 and (d) the Bragg peak intensity I as a function of the reduced temperature is shown. The solid lines are the best-fit results for fits to the power-law equations (3), (4) and (5) as described in the text.

law given in equation (5) using single values for the β-exponent and T_c. While the β-value in the range $T < T_L$ is close to the tri-critical value, the β-value in the range $T_L < T < T_c$ differs from all of the well known $d = 3$ model values, mean field ($\beta = 0.5$), Ising ($\beta = 0.33$), XY ($\beta = 0.35$) and Heisenberg ($\beta = 0.37$) [17]. Whether our experimental result for β is the true value in the asymptotic limit on approaching T_c is, as always in an experiment, open to question. In figure 4 we show the integrated intensity in the range $T_L < T < T_c$ on a log–log plot against reduced temperature, indicating the range of reduced temperatures over which we have measured. From the practical perspective, even if the critical region below T_c is very small in $NaNO_3$ and our results were not in the asymptotic limit, they still provide a good empirical representation of the behaviour of $NaNO_3$ in this temperature range.

4.3. Temperatures $T > T_c$

In this temperature range we have fitted the values for the inverse correlation lengths κ_c and κ_{ab} to the power law given in equation (3) and the values for susceptibility χ_0 to that given in equation (4). In these fits we kept T_c fixed at the value of 548.74 K obtained from the order parameter fits for consistency. The best-fit results are given in table 3 and are shown on the log–log plot of figure 4. The values for the exponent ν deduced from κ_c and κ_{ab} are similar and can be averaged to give an overall value of $\nu = 0.65 \pm 0.05$. When compared with the values for the various well known $d = 3$ model systems, mean field

($\nu = 0.5, \gamma = 1.0$), Ising ($\nu = 0.63, \gamma = 1.24$), XY ($\nu = 0.67, \gamma = 1.32$) and Heisenberg ($\nu = 0.71, \gamma = 1.39$) [17], the experimental values of $\nu = 0.65 \pm 0.05$ and $\gamma = 1.27 \pm 0.04$ are very similar to those of the Ising model. However, we note that while ν and γ obey within error the scaling relation $\gamma = (2 - \eta)\nu$ with η small (i.e. $\eta \sim 0$) [12, 17], the scaling relation $2\beta = d\nu - \gamma$ which links them with the β-value is only just satisfied within the limit of the error bars. In order to put this in context, it is worth remembering that for $d = 3$ this scaling relation would not be obeyed by the critical exponents for either mean-field or tri-critical behaviour. Hence if the value of β derived from the order parameter below T_c represents some form of crossover behaviour, then it may not be *a priori* true that this scaling relation should be satisfied anyway.

Apart from the exponent values, we can also compare the value for the ratio of the critical amplitudes $\kappa_c^+/\kappa_{ab}^+ = 8.52 \pm 2.29$ (cf. table 3) to the ratio of the inverse correlation lengths for the wide (temperature-independent) Lorentzian $\kappa_c/\kappa_{ab} = 11.58 \pm 1.31$ (cf. table 1). These are similar values, indicating that the two Lorentzians are subject to the same underlying asymmetry of the interatomic potential.

Table 3. The results for the critical exponents ν_c, ν_{ab} and γ obtained from fitting the values for κ_c, κ_{ab} and χ_0 at temperatures $T > T_c$.

	Exponent	Amplitude
χ_0	$\gamma = 1.27 \pm 0.04$	0.003 ± 0.001
κ_{ab}	$\nu_{ab} = 0.67 \pm 0.04$	0.48 ± 0.09
κ_c	$\nu_c = 0.63 \pm 0.04$	4.09 ± 0.79

5. Summary

The aim of the work presented in this paper was to examine the nature of the phase transition that occurs in sodium nitrate through the determination of the critical exponents ν, γ and β. Previous work by Schmahl and Salje [3] had shown that at a temperature $T \sim 460$ K (reduced temperature $t \sim 0.17$) the β-exponent describing the order parameter crossed over from a tri-critical value of $\beta = 0.25$ to a value of $\beta = 0.22 \pm 0.01$. We have examined the behaviour of the order parameter over a temperature range from 520 K up to $T_c = 548.75 \pm 0.47$ K and obtained values for the β-exponent in this range. Away from the transition, for temperatures $T < T_L$ our value of $\beta = 0.22 \pm 0.02$ with an effective transition temperature $T_c^* = 551 \pm 0.54$ K agrees well with the value of Schmahl and Salje [3]. However, for temperatures $T_L < T < T_c$ there is a distinct change in behaviour with a crossover to an exponent of $\beta = 0.41 \pm 0.02$ with a transition temperature $T_c = 548.75 \pm 0.47$ K.

At temperatures above T_c the scattering lineshape consists of two Lorentzian components, one of which is an effectively temperature-independent one. The other, temperature-dependent, component has been interpreted as being the critical scattering, and the temperature-independent component as being due to non-critical fluctuations. The critical scattering component has been analysed to yield values for the inverse correlation length and susceptibility, which in turn have been analysed to obtain the critical exponents $\nu = 0.65 \pm 0.05$ and $\gamma = 1.27 \pm 0.04$ respectively.

Acknowledgments

This work was supported by the United Kingdom Engineering and Physical Sciences Research Council under grant number GR/K-04989 and at the ISIS Facility. One of us (SJP) acknowledges the financial support of an EPSRC studentship and a CASE award from the Rutherford Appleton Laboratory. The crystal of $NaNO_3$ was kindly provided by the Chalk River Laboratories (Canada).

References

[1] Kracek F C 1931 *J. Am. Chem. Soc.* **53** 2609
[2] Dove M T and Powell B M 1989 *Phys. Chem. Minerals* **16** 503
[3] Schmahl W W and Salje E 1989 *Phys. Chem. Minerals* **16** 790
[4] Bruce A D and Cowley R A 1981 *Structural Phase Transitions* (London: Taylor and Francis)
[5] Harris M J, Salje E and Guttler B K 1990 *J. Phys.: Condens. Matter* **2** 5517
[6] Lynden-Bell R M, Ferrario M, McDonald I R and Salje E K H 1989 *J. Phys.: Condens. Matter* **1** 6523
[7] Shinnaka Y 1964 *J. Phys. Soc. Japan* **19** 1281
[8] Harris M J 1993 *J. Phys.: Condens. Matter* **5** 5773
[9] Schmahl W W, Pintchovius L and Fuess H 1989 *Z. Kristallogr.* **186** 261
[10] Dove M T, Hagen M E, Harris M J, Powell B M, Steigenberger U and Winkler B 1992 *J. Phys.: Condens. Matter* **4** 2761
[11] Hagen M, Dove M T, Harris M J, Steigenberger U and Powell B M 1992 *Physica* B **180+181** 276
[12] Cowley R A 1987 *Methods of Experimental Physics* vol 23, part C (New York: Academic) p 18
[13] Hagen M and Payne S J 1995 A guide to critical scattering measurements using time of flight neutron diffraction *Rutherford Appleton Laboratory Report* RAL-TR-95-034
[14] Payne S J, Hagen M E and Harris M J 1996 *J. Phys.: Condens. Matter* **8** 91
[15] Hagen M 1994 The PRISMA GENIE data analysis programs *Rutherford Appleton Laboratory Report* RAL-94-086
[16] Hagen M and Steigenberger U 1992 *Nucl. Instrum. Methods Phys. Res.* B **72** 239
[17] Collins M F 1989 *Magnetic Critical Scattering* (Oxford: Oxford University Press)
[18] Yeomans J M 1992 *Statistical Mechanics of Phase Transitions* (Oxford: Oxford Science Publications)